Application note

From waste to performance: Reactive extrusion upcycling validated by rheology and chemical (FTIR) imaging

Authors

Lucivan P Barros Jr & Ron L Rubinovitz
Thermo Fisher Scientific

Abstract

Polypropylene (PP) waste upcycling represents a strategic approach to reduce environmental stressors while generating value-added materials. In this study, reprocessed polypropylene (RPP) was incorporated into polyamide 12 (PA12) via reactive twin-screw extrusion using polypropylene grafted with maleic anhydride (PP-g-MA) as a compatibilizer. Morphology stabilization and interfacial adhesion were evaluated through oscillatory rheology, tensile mechanical testing, and micro-ATR Fourier transform infrared (FTIR) chemical mapping.

Reactive blends demonstrated increased storage modulus (G′), extended linear viscoelastic region (LVR), and recovery of tensile strength compared to non-reactive blends. Micro-ATR FTIR mapping provided quantitative assessment of phase homogeneity through polyamide-to-polypropylene peak area ratio analysis. Statistical evaluation confirmed a significantly narrower compositional distribution in compatibilized systems.

This integrated workflow demonstrates how the Thermo Scientific™ Process™ 11 Twin-Screw Extruder, Thermo Scientific™ HAAKE™ MiniJet Pro Injection Molding System, Thermo Scientific™ HAAKE™ MARS™ iQ Rheometer, and the Thermo Scientific™ Nicolet™ RaptIR™+ FTIR Microscope complement one another to enable efficient development and validation of upcycled polymer blends.

Introduction

Global plastic production exceeds 400 million tons annually, with polypropylene among the most widely used polymers. This high volume of polymer production results in large amounts of plastic ending up in our environment. Recycling is a strong potential solution; however, mechanical recycling often leads to molecular weight degradation via chain scission, limiting performance in secondary applications.

Upcycling through reactive extrusion provides a pathway to restore or enhance performance by incorporating recycled streams into high-value matrices. Polyamide 12 (PA12) offers superior mechanical and thermal properties but is immiscible with polypropylene due to thermodynamic incompatibility.

Compatibilization using PP-g-MA enables interfacial stabilization through in situ formation of diblock copolymers via reaction between maleic anhydride groups and PA12 amine end groups.

This study evaluates several aspects of the resultant plastic products:

- Molecular degradation of reprocessed PP
- Rheological signatures of interfacial stabilization
- Mechanical property recovery
- Quantitative chemical homogeneity via FTIR mapping

The role of screw design in reactive extrusion

The Thermo Scientific Process 11 twin-screw extruder was configured using a modular, co-rotating screw design to enable controlled melting, distributive mixing, and dispersive mixing within a single processing sequence. The initial feeding zone made use of conveying elements with relatively larger channel geometry to maximize solids intake and ensure stable material transport. This was followed by a plastification zone composed of forward-conveying mixing elements designed to progressively melt the polymers under controlled shear and thermal input. Downstream, the screw incorporated dedicated mixing sections where element geometry determined the dominant flow field imposed on the melt. Depending on the design and stagger angle of the kneading blocks, mixing elements can promote either distributive mixing, characterized by repeated division and recombination of melt streams without significant domain size reduction, or dispersive mixing, where higher shear stresses deform and break dispersed droplets into smaller domains.

The screws therefore impart distinct flow regimes, and variations in mixing type (distributive or dispersive) have been shown to significantly influence water absorption, blend microstructure, density, mechanical performance, and thermal behavior. In immiscible reactive blends, compatibilization reactions occur predominantly at the interface between phases. Thus, the degree of interfacial contact directly governs the extent of reaction between functional groups such as amine (-NH) and reactive anhydride or hydroxyl species. The distributive and dispersive mixing levels imposed by the screw profile strongly influence droplet size, morphology evolution, and total interfacial area. Since interfacial area determines the number of available reaction sites, screw configuration plays a critical role in controlling compatibilization efficiency and final blend morphology. The final conveying section stabilized melt pressure and ensured uniform delivery to the die, completing a screw architecture specifically tailored to maximize interface generation while preventing excessive degradation.[1] The evolution of phase morphology as a function of mixing type is schematically illustrated in Figure 1.

Figure 1. Schematic representation of morphology evolution in immiscible polymer blends (Polymer A + Polymer B) as a function of distributive and dispersive mixing intensity. Bottom left: limited distributive and dispersive mixing combined with poor interfacial stabilization results in droplet coalescence and the formation of large domains. Top left: insufficient distributive mixing leads to non-uniform spatial distribution of small domains within the matrix. Bottom right: effective distributive mixing achieves improved spatial homogeneity; however, inadequate dispersive mixing limits droplet size reduction. Top right: optimized distributive and dispersive mixing produce a stabilized morphology characterized by finely dispersed domains and uniform distribution. The balance between distributive and dispersive mixing directly governs droplet size, interfacial area generation, and overall compatibilization efficiency.

Materials and methods

Materials:

- Virgin polypropylene (vPP)
- Reprocessed polypropylene (rPP)
- Polyamide 12 (PA12)
- Polypropylene grafted maleic anhydride (PP-g-MA)

Blend compositions:

Blend composition	PA 12 (%)	rPP (%)	PP-g-MAH (%)
Reactive	50	40	10
Non-reactive	50	50	0

Table 1. Blend composition.

Processing was performed using a Process 11 twin-screw extruder with the following parameters:

- 11 mm co-rotating twin screws
- 40 L/D configuration
- Maximum 1000 rpm
- Temperature capability up to 450 °C
- Modular screw design enabling distributive and dispersive mixing

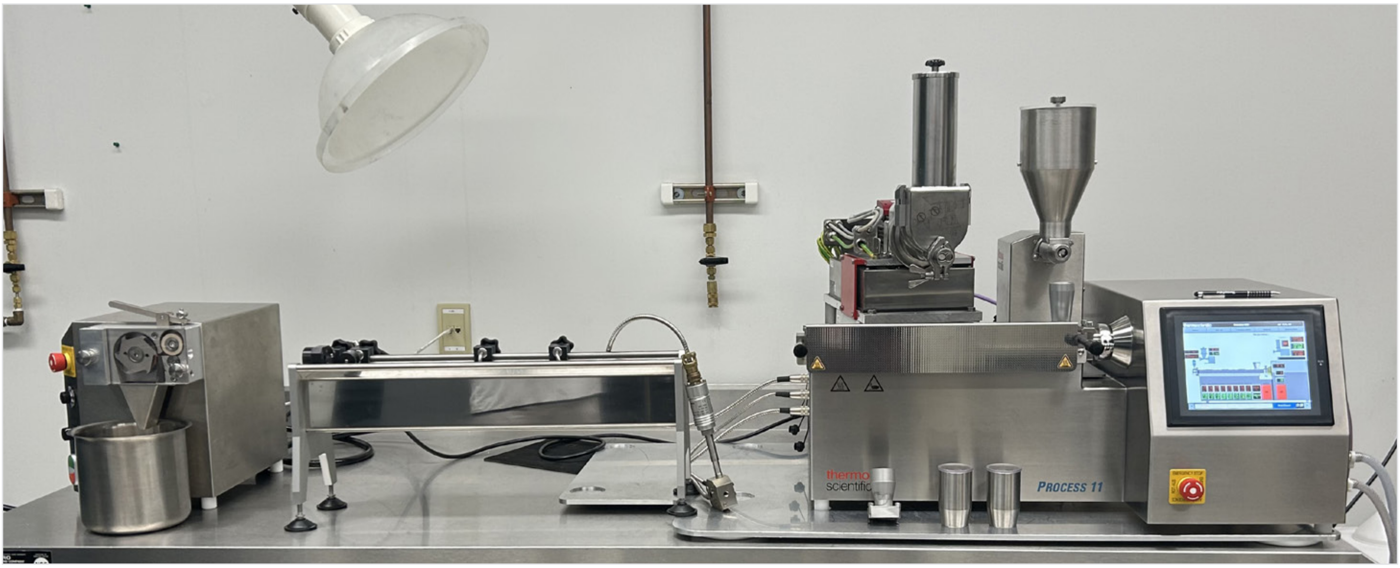

Figure 2. Thermo Scientific Process 11 with water bath and VariCut pelletizer setup.

The screw configuration included these zones:

- Feeding zone
- Melting/plastification zone
- Distributive mixing zone
- Dispersive mixing zone

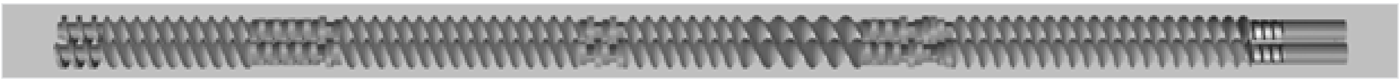

Figure 3. Process 11 screw configuration.

Virgin PP was first reprocessed under high shear to generate rPP.

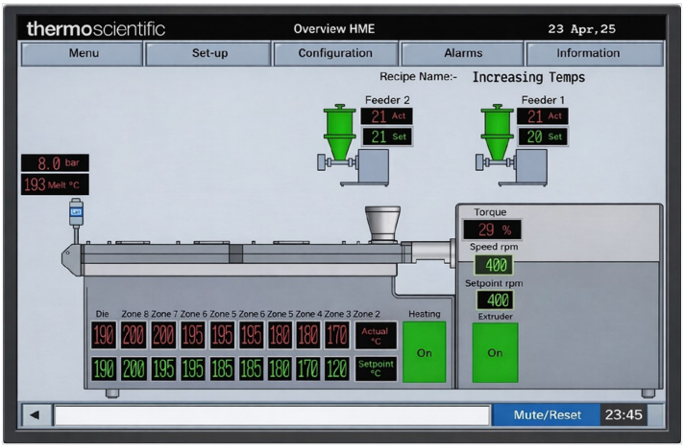

23 Apr,25

Recipe Name:- Increasing Temps

Feeder 2: 21 Act, 21 Set

Feeder 1: 21 Act, 20 Set

8.0 bar

193 Melt °C

Torque 29 %

Speed rpm 400

Setpoint rpm 400

Die	Zone 8	Zone 7	Zone 6	Zone 5	Zone 6	Zone 5	Zone 4	Zone 3	Zone 2
190	200	200	195	195	195	180	180	170	Actual °C
190	200	195	195	185	185	180	170	120	Setpoint °C

23:45

Figure 4. Process conditions and torque and die pressure during rPP production.

Specimens were molded using the HAAKE MiniJet Pro Piston injection molding system:

- 25 mm disc specimens for rheology
- Dog-bone specimens for tensile testing

Figure 5. HAAKE MiniJet Pro Piston injection molding system and molded specimens.

Rheological characterization was performed using oscillatory rheology. A HAAKE MARS iQ rotational rheometer was employed, measure key features.

- Parallel plate geometry
- Amplitude sweep (LVR determination)
- Frequency sweep (viscoelastic response)

Figure 6. HAAKE™ MARS™ iQ Rotational Rheometer.

Mechanical testing was used to evaluate tensile characteristics:

- Young’s modulus
- Tensile strength
- Yield stress
- Yield strain

FTIR microscopy and chemical mapping

While rheological and mechanical testing provide indirect evidence of interfacial stabilization, direct chemical verification of phase distribution is required to confirm compatibilization efficiency. Immiscible polymer blends such as PP/PA12 exhibit morphology-dependent performance governed by droplet size, spatial distribution, and interfacial adhesion.

Micro-ATR Fourier transform infrared (FTIR) spectroscopy enables spatially resolved chemical analysis without extensive sample preparation. The Nicolet RaptIR+ FTIR microscope was used to collect high-density chemical maps of blend cross-sections, providing direct insight into compositional uniformity and interfacial mixing.

ATR sampling was selected to minimize preparation artifacts and avoid the need for thin microtomed sections. The evanescent wave penetration depth of less than a few microns enables surface-sensitive chemical characterization while maintaining high spectral quality.

To enable quantitative phase mapping, distinct and non-overlapping spectral markers were selected:

- PA12 amide I band (~1636 cm^{-1}) – characteristic carbonyl stretch of polyamide
- PP methyl deformation (~1376 cm^{-1}) – characteristic polypropylene signature

These bands were chosen for specific reasons:

- High intensity
- Minimal overlap
- Structural specificity

A peak area ratio (PA12/PP) was calculated for each spectrum within the map to eliminate intensity variations due to contact differences or sampling conditions. This ratio serves as a local compositional indicator and enables quantitative comparison across the mapped area.

More than 1000 spectra were collected per mapped region, ensuring statistical robustness. Mapping was performed at spatial resolutions down to 10 × 10 µm, approaching the expected droplet size scale.

The large number of spectra enables transformation of chemical imaging into a quantitative dataset rather than a qualitative visualization. Each measurement point contributes to a compositional distribution profile, allowing extraction of important information:

- Minimum and maximum ratio values
- Range
- Standard deviation
- Histogram distribution

This approach provides objective metrics of phase homogeneity.

Figure 7. Nicolet RaptIR+ FTIR Microscope (right) connected to Nicolet iS50 FTIR Spectrometer (center) configured with built-in diamond ATR module, ABX Automated Beamsplitter Exchanger Tower Unit and FT-Raman module, and attached to an NIR module with integrating sphere (left).

Results and discussion

Virgin polypropylene (vPP) was subjected to reprocessing under high shear conditions (400 rpm, ~40 s residence time) using a temperature profile increasing from 120 °C (Zone 1) to 200 °C (Zone 8), with a die temperature of 190 °C. Under these conditions, thermo-mechanical degradation via chain scission is expected, particularly in the presence of oxygen traces and high shear stress.

Polymer melts are non-Newtonian fluids that typically exhibit shear thinning, where viscosity decreases as shear rate increases. While steady-state rotational shear is often used for polymer solutions, polymer melts are better characterized using small amplitude oscillatory shear due to their elasticity and sensitivity to deformation.[2]

Using the Cox–Merz rule, the complex viscosity obtained from oscillatory measurements can be related to steady-state shear viscosity. As a result, oscillatory frequency sweeps are the preferred method for determining apparent shear viscosity in molten polymers (Figures 8 and 11). [2,3]

Oscillatory rheology performed at 180 °C clearly revealed the effect of reprocessing on molecular architecture. In amplitude sweep measurements, vPP exhibited a higher storage modulus (G′) plateau compared to reprocessed polypropylene (rPP), indicating a greater entanglement density and higher molecular weight. The reduction in plateau modulus for rPP is consistent with decreased chain length due to scission events.

Frequency sweep analysis further confirmed this behavior. (See Figure 9.) vPP displayed higher G′ and G″ values across the measured frequency range (10–100 Hz), along with increased complex viscosity. In entangled polymer systems, viscosity scales approximately with molecular weight to the power of 3.[4]. Therefore, even modest chain scission significantly reduces viscoelastic response. The reduced relaxation time spectrum observed in rPP suggests fewer long-chain entanglements capable of storing elastic energy.

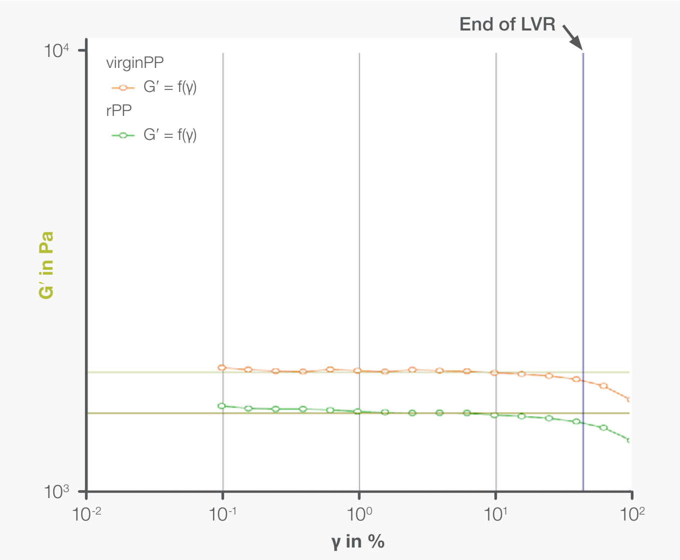

Figure 8. Amplitude sweeps of vPP (black) and rPP (green).

Differential scanning calorimetry (DSC) also showed a decrease in crystallinity from 63.1% (vPP) to 58.1% (rPP). Chain scission can disrupt optimal lamellar folding and crystalline perfection, slightly lowering crystallinity while also potentially increasing chain mobility in the amorphous phase.

Collectively, rheological and thermal data confirm that the reprocessing protocol successfully generated a degraded polypropylene stream suitable as a realistic recycled feedstock.

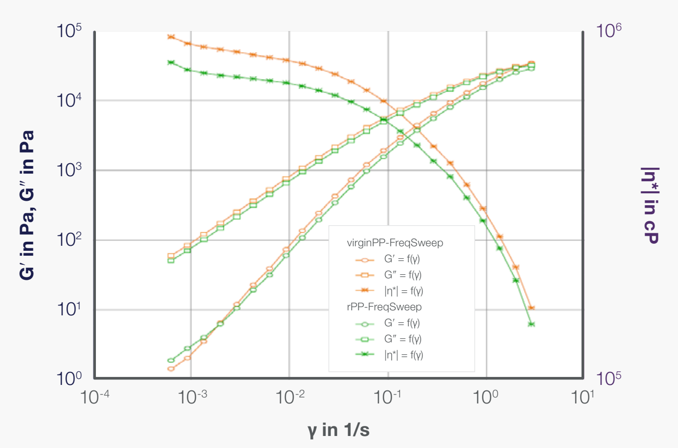

Figure 9. Frequency sweep of vPP and rPP.

Interfacial engineering via reactive extrusion

Reactive and non-reactive blends were compounded under identical Process 11 extruder conditions (400 rpm, identical thermal profile, ~40 s residence time), isolating chemistry as the key variable. No torque increase or crosslinking was observed, indicating that compatibilization occurred primarily at the interface without bulk gel formation.

In the reactive system, polypropylene grafted with maleic anhydride (PP-g-MA) reacted in situ with terminal amine groups of PA12 during extrusion (185–200 °C), forming interfacial copolymers as illustrated in Figure 10. These species reduce interfacial tension and suppress droplet coalescence.

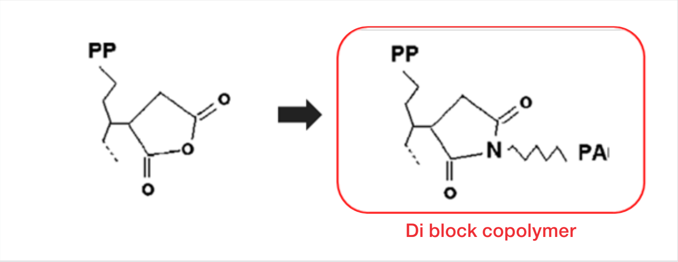

Figure 10. Scheme of blend compatibilization reaction with the formation of a di-block copolymer of PP and PA12.[4]

An interesting macroscopic observation supporting improved interfacial behavior was improved pellet cutting during pelletization of the reactive blend. Cleaner cutting behavior suggests a more cohesive and uniform melt strand, consistent with improved phase interaction and reduced weak interfacial discontinuities. The modular screw design of Process 11, which incorporates distributive and dispersive mixing zones, enabled efficient interface generation, while chemical compatibilization stabilized the morphology.

Rheological signatures of compatibilization

Rheological testing of blends was conducted in amplitude (strain amplitude range 0.1-100.0 % and frequency at 1.0 Hz) and frequency sweep (strain amplitude 1.0%, frequency range 0.01–100.0 Hz) at 180 °C for vPP and rPP and 220 °C for the blends. (Refer to Figures 11 and 12.)

Amplitude sweep: Interfacial elastic reinforcement

The reactive blend exhibited a significantly higher storage modulus (G′) across the linear viscoelastic region (LVR) compared to the non-reactive blend. Additionally, the LVR extended to higher strain values in the reactive system.

In immiscible blends, the interface contributes to viscoelastic behavior. A stabilized interface with copolymer anchoring increases resistance to deformation because interfacial slippage is reduced. The longer LVR in the reactive blend indicates that the interfacial network tolerates larger deformations before structural breakdown, reflecting enhanced stress transfer between phases.

In contrast, the non-reactive blend exhibited earlier deviation from linearity, suggesting weak interfacial adhesion and easier debonding under strain.

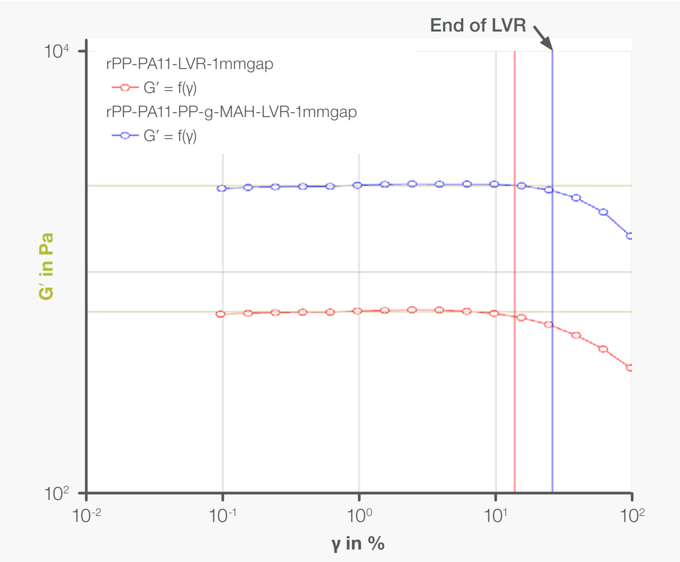

Figure 11. Amplitude sweep of reactive (blue) and non-reactive (red).

Frequency sweep: Relaxation dynamics

In frequency sweeps, the reactive blend displayed elevated G′ values, particularly toward the lower frequency region. Increased low-frequency elasticity is often associated with constrained relaxation mechanisms and interfacial elasticity in multiphase systems.[5]

In non-reactive blends, dispersed domains relax independently, leading to faster stress relaxation. However, when compatibilized, interfacial copolymers restrict droplet mobility and suppress coalescence-driven relaxation, shifting the relaxation spectrum toward longer times.[6]

This rheological behavior provides indirect but strong evidence of interfacial stabilization via reactive compatibilization.

The MARS iQ Air platform enables sensitive detection of these interfacial viscoelastic signatures.

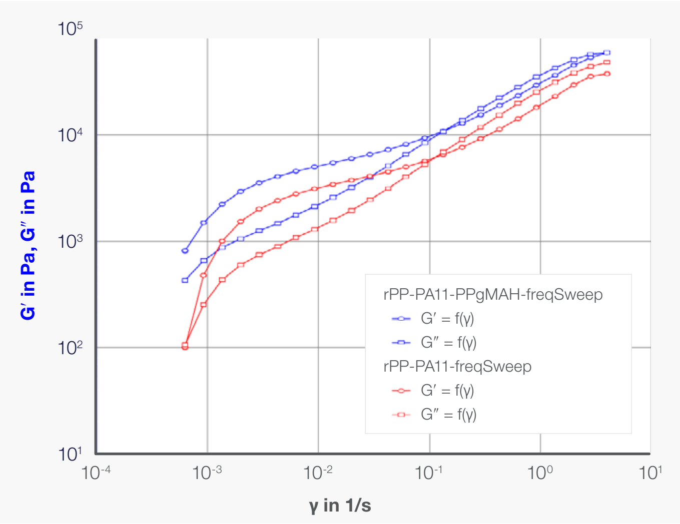

Figure 12. Frequency sweep of reactive and non-reactive blend.

Structure–property correlation from mechanical testing

Mechanical specimens prepared using the HAAKE MiniJet Pro injection molding system enabled controlled evaluation of structure–property relationships (see Figure 13). Here mechanical tests were performed in neat/virgin PA12 and on reactive and non-reactive blends.

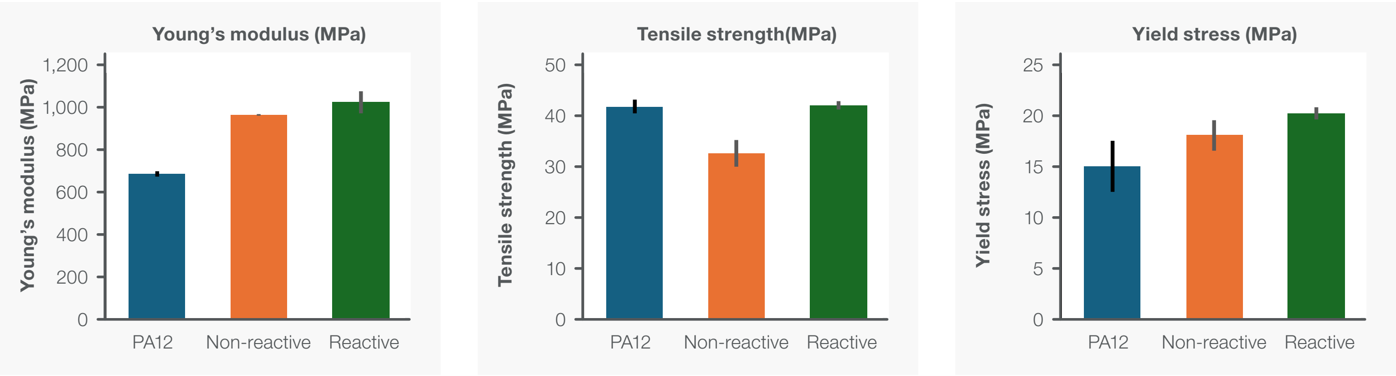

Figure 13. Mechanical properties of the blends and neat polyamide 12.

Modulus enhancement

Both blends exhibited significantly higher modulus than neat PA12. The increase arises from incorporation of the semi-crystalline polypropylene phase, which acts as a reinforcing component. Additionally, DSC revealed increased crystallinity in the reactive blend (39.7%) compared to the non-reactive blend (35.1%), contributing to stiffness enhancement.

Tensile strength: Interfacial failure mechanism

The non-reactive blend showed a substantial tensile strength reduction (32.49 MPa vs 41.76 MPa for PA12). This is characteristic of immiscible blends with weak interfaces, where stress concentration at phase boundaries initiates premature crack propagation.

In contrast, the reactive blend recovered tensile strength (41.94 MPa), essentially matching neat PA12 despite containing 50% recycled PP. This indicates effective stress transfer across the interface and suppression of debonding mechanisms.

Yield behavior

Yield stress increased progressively from PA12 to reactive blend (15.01 → 20.20 MPa). Increased yield stress reflects improved load distribution and restricted plastic deformation due to enhanced phase adhesion and modified crystallinity.

Correlation with rheology and mechanical performance

The chemical homogeneity observed in reactive blends directly correlates with multiple qualities:

- Increased G′ plateau modulus
- Extended linear viscoelastic region
- Recovery of tensile strength to PA12 levels
- Increased yield stress

Uniform phase distribution increases interfacial area while preventing stress concentration sites. Interfacial copolymer formation restricts droplet coalescense and enhances stress transfer, explaining the rheological signatures observed.

Quantitative chemical mapping by micro-ATR FTIR

Spectral identification of base materials

The FTIR spectra of the base materials, polypropylene, and PA12 were measured by the micro-ATR (attenuated total reflectance) technique using a germanium crystal. The spectra obtained demonstrated the expected characteristic differences between these two polymers. Strong unique peaks at 1636 cm^{-1} and 1376 cm^{-1} for PA12 and polypropylene, respectively, can be clearly seen (Figure 14).

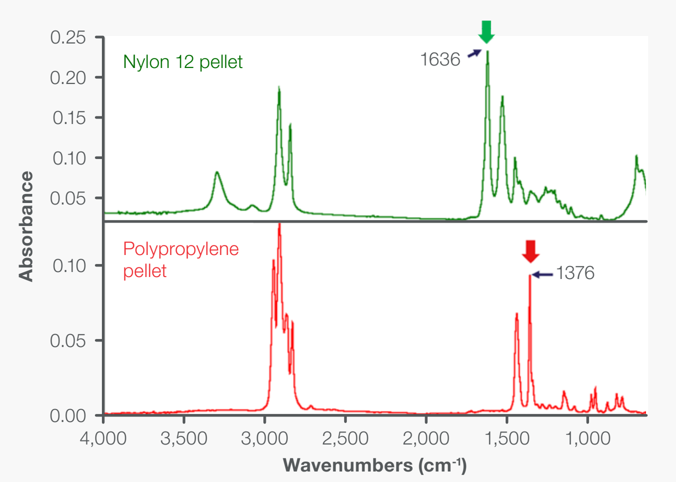

Figure 14. Comparison of the ATR spectra of PA12 and polypropylene, showing unique spectral features.

Micro-ATR maps were collected using the exposed cross sections of reactive blend and non-reactive blend pellets containing 10% or 0% PP-g-MA, respectively. Over 1000 spectra at 8 cm^{-1} resolution and 64 scans for each spectrum were collected for each map. Results presented here were collected with a 10x10 micron measurement area for each spectrum. Individual map spectra contained contributions from both PP and PA12; however the non-reactive pellet map showed dramatically different ratios of PP to PA12 across its surface. Representative spectra demonstrating the variation seen in the collected spectra are shown in Figure 15.

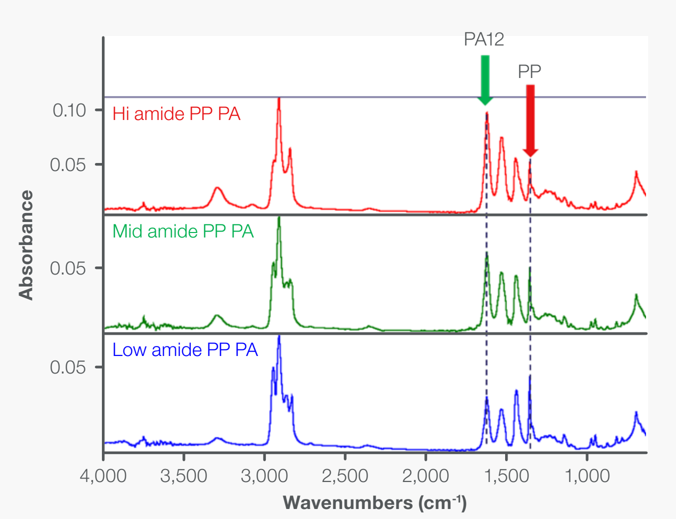

Figure 15. Map spectra collected from high, intermediate and low amide regions in the non-reactive blend sample.

Quantitative ratio-based analysis

In order to assess the degree of blending, the ratio of the area under the PA12 peak, between 1680 and 1610 cm^{-1} and the area under the PP peak between 1390 and 1345 cm^{-1} was calculated for each map spectrum (Figure 16). Ratio values for various measured spectra are shown in Figure 17.

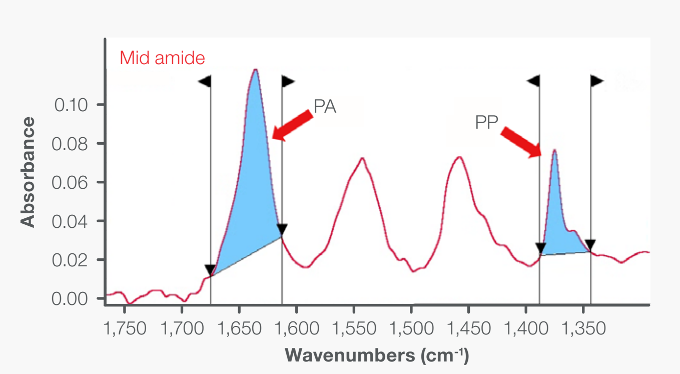

Figure 16. Spectral regions used for area ratio calculation.

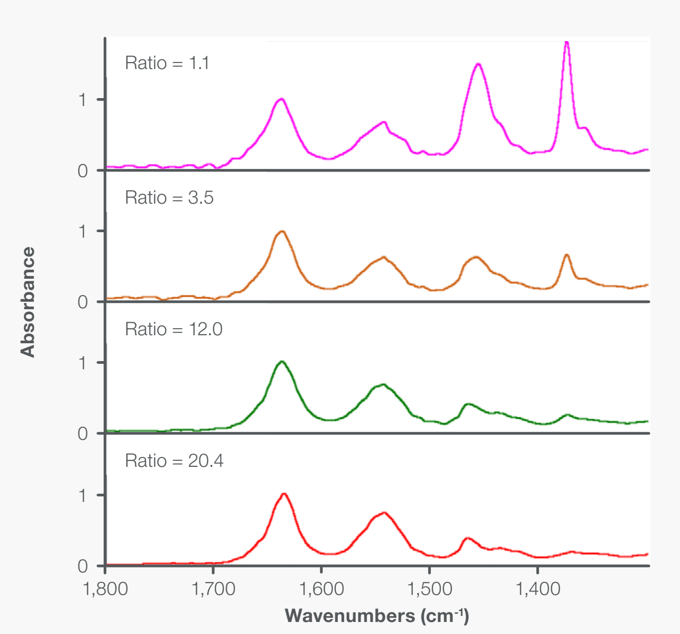

Figure 17. Examples of varying ratios between PA12 and PP spectral features with area ratios shown. Spectra have been baseline corrected and normalized to the amid I peak of PA12 at 1640 cm^{-1}.

Distribution of phases within maps

Comparing the maps collected for non-reactive and reactive blends shown in Figure 18 demonstrate the clear differences between the ratio values of the two samples. A more quantitative comparison between the two maps was carried out by straight forward statistical analysis. While the reactive blend map had ratio values ranging from 2.6 to 4.8 (standard deviation=0.306), the non-reactive blend had ratio values ranging from 1 to 12 (standard deviation=1.65). The wide distribution of the non-reactive blend is indicative of large phase domains and incomplete mixing. Further, the presence of near-pure domains in the non-reactive blend (~1% of mapped area) indicates insufficient interfacial stabilization, consistent with rheological and mechanical results.

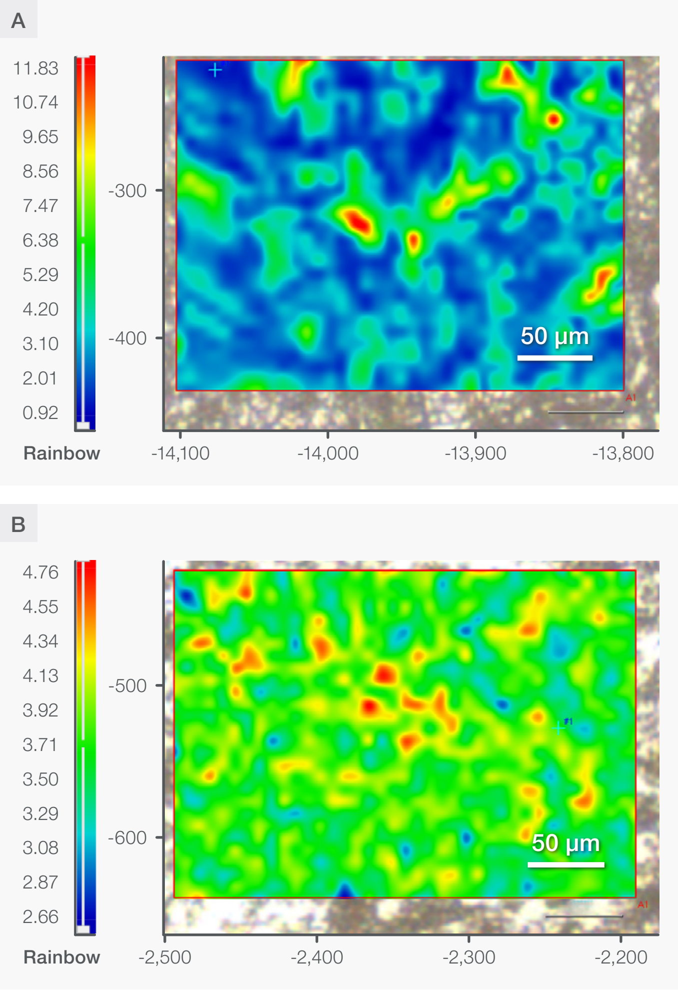

Figure 18. Chemical maps of the non-reactive blend (A) and reactive blend (B), demonstrating significantly less blending variation in the reactive blend sample.

Statistical evaluation of blend homogeneity

The analysis of the ratio values also included a comparison of the histogram of the ratio values within each map (Figure 19), clearly showing significantly less variation (better blending) within the reactive blend sample. The wide distribution seen in the non-reactive blend sample is indicative of heterogenous morphology and poor mixing. Alternatively, the narrow distribution observed for the reactive blend demonstrated homogeneous morphology and effective compatibilization. Even at 10 µm resolution, spectra from the reactive mixture consistently contained contributions from both polymers, implying domain sizes below the spatial resolution limit.

Importantly, statistical FTIR analysis provides a process optimization metric. Instead of relying solely on qualitative maps, histogram width and standard deviation can serve as measurable indicators of compatibilization efficiency and process robustness.

The FTIR mapping results provide direct chemical confirmation of the trends observed in rheological and mechanical testing.

The broad compositional distribution in the non-reactive blend correlates with several disadvantageous features:

- Lower tensile strength due to stress concentration at poorly bonded interfaces
- Reduced LVR and faster relaxation behavior in rheology
- Weak interfacial adhesion

In contrast, the uniform composition observed in the reactive blend aligns with more desirable attributes:

- Increased storage modulus (G′) and extended LVR
- Recovery of tensile strength to PA12 levels
- Improved yield stress and overall mechanical integrity

The absence of pure-phase domains and the reduced compositional variability indicate that compatibilization effectively increases interfacial area and promotes efficient stress transfer between phases.

Beyond qualitative visualization, micro-ATR FTIR mapping combined with statistical analysis provides a powerful quantitative tool for process optimization. Metrics such as ratio range and standard deviation can be directly linked to processing parameters, including screw configuration, mixing intensity, and compatibilizer concentration.

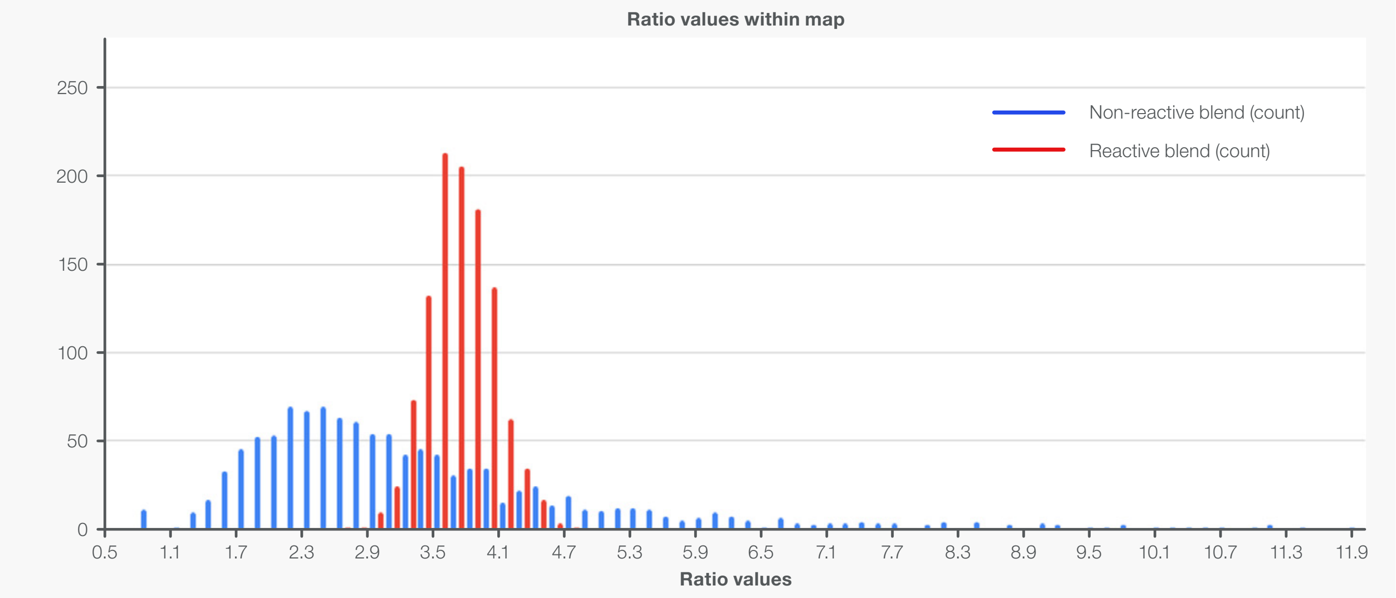

Figure 19. Distribution of ration values within each map, showing significantly less variation in the non-reactive sample.

Conclusion

Reactive extrusion of reprocessed polypropylene with PA12 using PP-g-MA successfully produced a mechanically robust upcycled material containing 50% recycled content.

Key outcomes:

- Rheology confirmed enhanced interfacial stability.
- Tensile properties were restored to near-virgin PA12 performance.
- FTIR chemical mapping provided quantitative compositional uniformity analysis.
- Statistical treatment of mapping data enabled objective evaluation of compatibilization efficiency.

The integrated workflow combining extrusion, molding, rheology, and FTIR microscopy enables accelerated development of sustainable polymer blends with validated performance.

References:

1. On-line ATR-MIR for real-time quantification of chemistry kinetics along the barrel in extrusion-based processes - ScienceDirect
2. Thermo Fisher App note AN56376 – Nathan C. Crawford. Examining the rheological behavior of three nearly identical linear low-density polyetheylene (LLDPE) samples.
3. W.P. Cox and E.H. Merz. Correlation of dynamic and steady flow viscosities. Journal of Polymer Science, 28, 619 (1958).
4. Effect of PP-g-MAH compatibilizer content in polypropylene/nylon-6 blends | Polymer Bulletin | Springer Nature Link
5. Hyung Gon Lee, Yu-Taek Sung, Yun Kyun Lee, Woo Nyon Kim, Ho Gyu Yoon, and Heon Sang Lee. Effects of pp-g-mah on the mechanical, morphological and rheological properties of polypropylene and poly(acrylonitrile-butadiene-styrene) blends, 2009.
6. Effect of different polypropylenes and compatibilizers on the rheological, mechanical and morphological properties of nylon 6/PP blends | Journal of Materials Science | Springer Nature Link

Learn more at **thermofisher.com/ftir**

MCS-AN1803-EN 5/26